Microstructure and Mechanical Properties of Duplex Structured Mg-Li-Zn-Y Alloys

J-f. Su [a], Y. Yang *, [a, b], X-s. Fu [a], Q-y. Ma [a], F-j. Ren [a], X-d. Peng [a, b]

[a] College of Materials Science and Engineering, Chongqing University, Chongqing, 400044, China
[b] National Engineering Research Center for Magnesium Alloys, Chongqing 400044, China
*Corresponding author. E-mail address: yanyang@cqu.edu.cn

Abstract

As-cast Mg-6Li-0.3Zn-0.6Y and Mg-6Li-1.2Zn-1.2Y (wt%) alloys were prepared and extruded at 260 $^{\circ}$C with an extrusion ratio of 25. The microstructure and mechanical behavior of as-cast and extruded alloys are reported and discussed. The results show that Mg-6Li-1.2Zn-1.2Y alloy is composed of α-Mg, β-Li, and W-$Mg_3Zn_3Y_2$ phases while Mg-6Li-0.3Zn-0.6Y alloy contains α-Mg, β-Li, W-$Mg_3Zn_3Y_2$ phase and X-$Mg_{12}ZnY$. After hot extrusion, the microstructure of specimens is refined and the average grains size of extruded alloys is 15 μm. Dynamic recrystallization occurs during the extrusion, leading to grain refinement of test alloys. Both the strength and elongation of test alloys are improved by extrusion. The extruded Mg-6Li-0.3Zn-0.6Y alloy possesses an ultimate strength of 225 MPa with an elongation of 18% while the strength and elongation of Mg-6Li-1.2Zn-1.2Y alloy are 206 MPa and 28%, respectively. The X-phase in Mg-6Li-0.3Zn-0.6Y is beneficial to the improvement of strength, but will lead to the decrease of ductility.

Keywords: Mg-Li-Zn-Y alloy, Microstructure, Mechanical properties, Extrusion

1. Introduction

Mg-Li alloys, as the lightest metal structural materials, have drawn extensive research interest. Mg-Li alloys are being used to speed up the process of lightweight in aerospace, automotive, electrical and military field due to their low density, high specific strength and elastic modulus, good electromagnetic shielding and machining property [1,2].

The crystal structure of Mg-Li alloy is different with the change of lithium content. The Mg-Li phase diagram [3] indicates that when Li content is between ~5.7 and 10.3 wt%, a duplex structure alloy with eutectic microstructure is formed containing both hcp structured α-Mg phase and bcc structured β-Li phase. And it is also believed that dual-phase Mg-Li alloys can exhibit good ductility while maintaining relatively high strength at the same time [4]. However, the strength, corrosion and creep resistance of Mg-Li alloys are very low due to the addition of Li. Generally, previous strengthening methods, such as adding Zn or Al alloying elements and severe plastic deformation, cannot make the ultimate tensile strength of Mg-Li alloys exceed 200 MPa [5], which limits their widespread application. On the other hand, it has been reported that Mg-Zn-Y alloys containing X-phase ($Mg_{12}ZnY$, long period stacking structure) and I-phase (Mg_3Zn_6Y, icosahedral quasicrystal structure) as a secondary phase exhibit high strength at room temperature [6,7].

Although it has been reported that there exists a two-phase region consisted of X-phase and α-Mg in the Mg-rich composition range of the Mg-Zn-Y system, there has been little report on the effect of Zn and Y addition on the microstructure and mechanical properties of duplex structured Mg-Li-Zn-Y alloys. Therefore, in the present study, we have examined the change of the microstructure depending on the ratio of Zn/Y in the composition range.

The previous investigations [8] also indicated that the increasing of α-phase fraction in dual-phase Mg-Li alloys will lead

to an increase of strength. When the Li proportion of duplex Mg-Li alloys is near 5.7 wt%, the α-phase fraction of the alloy will reach a high level, which has the latency to develop high strength Mg-Li alloys without sacrificing too much plasticity.

Based on the analysis mentioned above, two alloys (with different Zn/Y ratios), namely Mg-6Li-0.3Zn-0.6Y (wt%) and Mg-6Li-1.2Zn-1.2Y (wt%), were prepared in this work.

2. Materials and experimental procedures

Alloys with different Y/Zn ratio were prepared from Mg (purity 99.9%), Li (purity 99.9%), Zn (purity 99.9%) and Mg-30Y master alloys in a carbon crucible under the protection of a mixed atmosphere of SF_6 (10%, volume fraction) and CO_2 .

Pure Mg, pure Zn and Mg-30Y master alloy were melted at 720 ^oC and then pure Li was added by an inverted mild steel cup. After the melt was kept at 720 ^oC for 10 min, it was cast into a cylinder metal mold preheated to 200 ^oC with the ingot size of Φ90×300 mm. The as-cast ingots (machined to Φ80×50 mm) was then homogenization treated at 260 ^oC for 1 h and extruded into a long rod with a diameter of 16 mm (extrusion ratio was 25:1) at the temperature of 260 ^oC .

Inductively coupled plasma-atomic emission spectrometer (ICP-AES) was applied to determine the chemical compositions of the alloys, and the results are listed in Table 1. The microstructures were examined by optical microscopy (OM), scanning electron microscopy (SEM) equipped with energy dispersive spectrometer (EDS) .The samples were etched by nitric acid ethanol solution (2 ml nitric acid, 50 ml ethanol). X-ray diffraction analysis (XRD) was used to determine the phases of the alloys.

Table 1.
Actual chemical compositions of experimental alloys (mass fraction, %)

Alloys	Chemical composition (wt. %)				Zn/Y ratio
	Li	Zn	Y	Mg	
Mg -6Li -0.3Zn -0.6Y	6.06	0.34	0.59	Bal.	0.58
Mg -6Li -1.2Zn -1.2Y	5.93	1.18	1.20	Bal.	0.98

Tensile specimens with gauge dimensions of Φ5×25 mm were machined from the central regions of the extruded samples. Tensile tests were carried out on a CMT-5105 (SANS Materials Analysis Inc., Shenzhen, China) tensile tester with a displacement speed of 2 mm/min at room temperature.

3. Results and discussion

3.1. Microstructure of as-cast alloys

The as-cast structure of the alloys presents a dual-phase microstructure, as given in Fig. 1. It can be seen that these alloys are mainly made up of α-Mg phase. The α-Mg phases of alloys are mainly dendrite, and the β-Li phase shows to be of small fraction and divides α-Mg phase into parts. It also shows that the second-phase particles distributed along phase boundaries in both two alloys. The β-phase is the Li solid solution of low atomic number while the α-phase is the Mg solid solution with a higher atomic number. It also shows that the second-phase particles distributed along phase boundaries in both two alloys.
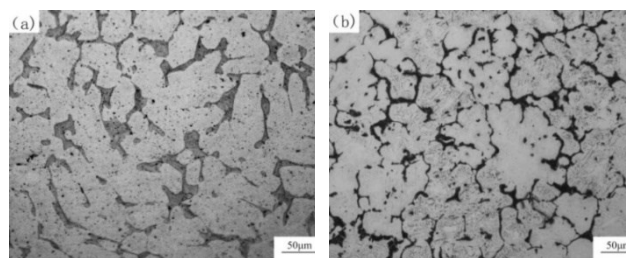

Fig. 1. Optical microstructure of as-cast specimen: (a) Mg-6Li-0.3Zn-0.6Y alloy; (b) Mg-6Li-1.2Zn-1.2Y alloy

Fig. 2 shows the XRD pattern of as-cast Mg-6Li-0.3Zn-0.6Y and Mg-6Li-1.2Zn-1.2Y. The pattern indicates that the Mg-6Li-0.3Zn-0.6Y alloy is consists of α-Mg, β-Li, W-$Mg_3Zn_3Y_2$ (cubic structure), and X-$Mg_{12}ZnY$ (a long-period 18R modulated structure). However, there is no X-$Mg_{12}ZnY$ in Mg-6Li-1.2Zn-1.2Y alloy. The XRD analysis reveals that the change of alloy composition is mainly determined by the content and ratio of Zn and Y.
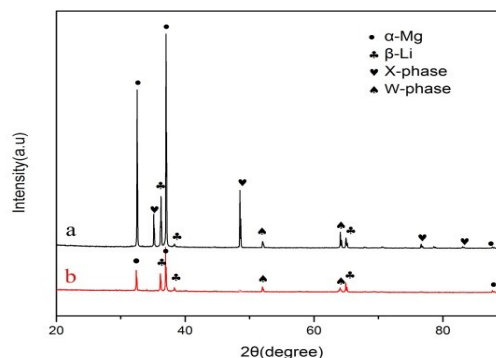

Fig. 2. XRD patterns of as-cast specimen: (a) Mg-6Li-0.3Zn-0.6Y alloy; (b) Mg-6Li-1.2Zn-1.2Y alloy

In order to characterize the microstructure of the alloys more clearly and make sure the composition of the compound, the SEM and EDS energy spectrum analysis were carried out. The SEM images of as-cast alloys are shown in Fig. 3.As can be seen from Fig. 3 that white second-phase particles in alloys are mainly distributed at the interface of α-Mg/β-Li, which is consistent with

the above analysis. But it is worth noting that the second-phase particles can also be observed inside matrix in Mg-6Li-0.3Zn-0.6Y alloy. So, it indicates that there is a correlation between the distribution of second phase and the segregation of yttrium and zinc in Mg-Li alloys.
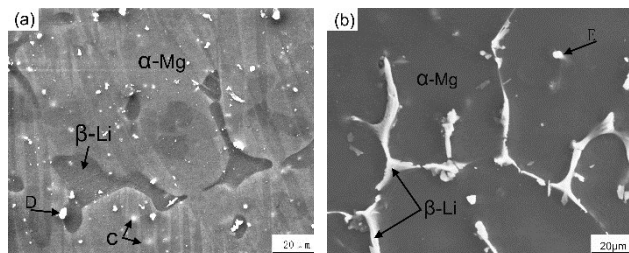

Fig. 3. SEM images of as-cast specimen: (a) Mg-6Li-0.3Zn-0.6Y alloy; (b) Mg-6Li-1.2Zn-1.2Y alloy

The element contents of bright white particles (labeled as C, D and E) in Fig. 3 are analyzed by EDS. The element contents are given in Table 2. Since Li element cannot be detected, Li content is not included in this table.

Table 2.
Chemical composition distribution of as-cast Mg-Li-Zn-Y alloys

Content	Point		
%	C	D	E
Mg	83.7	96.5	91.1
Zn	7.9	1.9	5.2
Y	8.4	1.6	3.7
Totals	10	10	10

The EDS results show the composition of particle C is enriched in Mg, Zn and Y elements. And the atom amount ratio of Zn to Y is close to 1:1. Combined with XRD analysis results, it can be concluded that the phase of particle C is X-$Mg_{12}ZnY$ accordingly. Meanwhile, the EDS analysis shows that the atom amount ratio of Zn to Y in particle C and D are both close to 3:2. Luo Suqin et al. [9] investigated effect of mole ratio of Y to Zn on phase constituent of Mg-Zn-Zr-Y alloys indicated that there is W-phase (($Mg_3Y_2Zn_3$)) in Mg-Zn-Y (-Zr) system alloys when the mole ratio of Zn to Y is in the range of 0.75~3.22. It illustrates that the white tiny particle C and D are $Mg_3Y_2Zn_3$ phases.

3.2. Microstructure of as-extruded alloys

Fig. 4 shows the microstructure of as-extruded alloys with extrusion ratio of 25. It can be seen that the grain size in the extruded specimen is relatively finer as compared to as-cast specimen. It is also apparent that α-Mg phase is elongated, becoming long strips parallel to the extrusion direction. However, β-Li phase shows big difference microstructure characteristics with α-Mg. As shown in the Figs.4 (c) and (d), β-Li phase exhibits equiaxed morphology with a grain size of smaller than 5μm while α-Mg phase is only elongated along the extrusion direction. Therefore, it indicates that the α-Mg and β-Li phases exhibit different mechanisms of microstructure evolution during the hot extrusion process.
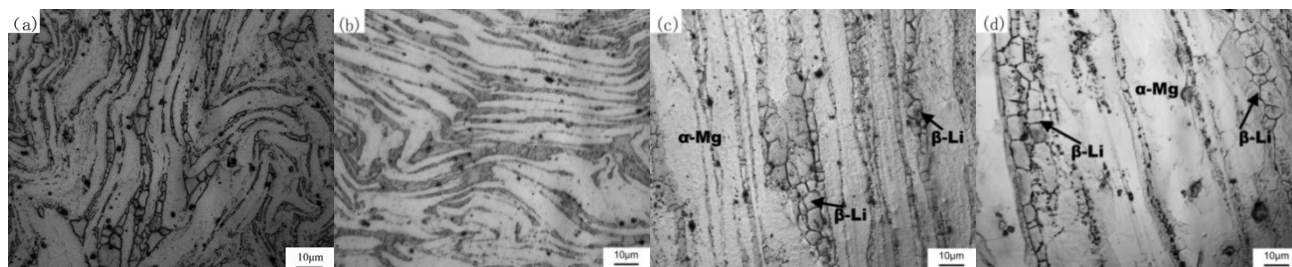

Fig. 4. OM images of as-extruded specimen: (a) Mg-6Li-0.3Zn-0.6Y alloy, vertical to extruding direction;
(b) Mg-6Li-1.2Zn-1.2Y alloy, vertical to extruding direction; (c) Mg-6Li-0.3Zn-0.6Y alloy, parallel to extruding direction;
(d) Mg-6Li-1.2Zn-1.2Y alloy, parallel to extruding direction.

YI S B et al. [10] investigated mechanical behavior and microstructure evolution of magnesium alloy AZ31 in tension at different temperatures indicated that CDRX is the dominant mechanism for microstructural refinement in α-Mg phase at the extrusion temperature of 260 ^{o}C with an extrusion ratio of 25. Respectively, the microstructural features observed from SEM for β-Li phase are consistent with the microstructural characteristics widely reported for DDRX. Usually, DDRX is promoted at relatively high temperatures and in order to accelerate the development of DDRX, some deformation is usually necessary. During hot extrusion deformation process, a plastic deformation occurs first in the β-Li phase for the ductility of β-Li phase (bcc

structure) is better than α-Mg phase (hcp structure). Apart from that, the melting point of the β-Li phase is relatively low (588 ^{o}C in eutectic region), thus the extrusion temperature of 260 ^{o}C is high enough to meet the temperature requirement of DDRX.
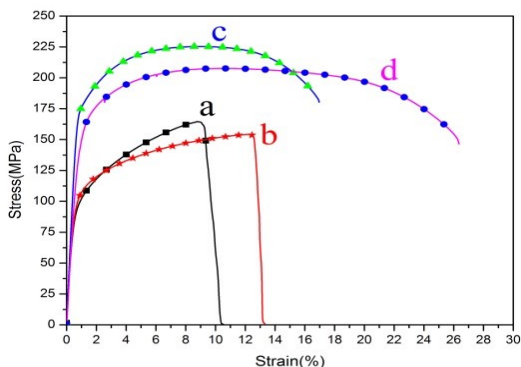
3.3. Mechanical properties of alloys

Fig. 5. Tensile stress-strain curve of specimen: (a) as-cast Mg-6Li-0.3Zn-0.6Y alloy; (b) as-cast Mg-6Li-1.2Zn-1.2Y alloy; (c) as-extruded Mg-6Li-0.3Zn-0.6Y alloy; (d) as-extruded Mg-6Li-1.2Zn-1.2Y alloy

The stress–strain curves are shown in Fig. 5. To describe and compare these conveniently, the mechanical properties of 0.2% proof yield stress ($\sigma_{0.2}$), UTS and elongation to failure for the alloys are listed in Table 3.

It can be seen that the strength and ductility of the two alloys were both improved greatly after extrusion deformation. This may be attributed to the reduction of shrinkage porosity, slag inclusion and so on in the extruded specimen. Moreover, the grain refinement both in α-Mg and β-Li phases also plays an important role in enhancing the mechanical properties of extruded alloys.

In comparison with the alloys, the mechanical properties of extruded Mg-6Li-0.3Zn-0.6Y are quite different from Mg-6Li-1.2Zn-1.2Y. The extruded Mg-6Li-1.2Zn-1.2Y alloy has excellent ductility with the elongation of 28%. Its strengths are comparatively low with $\sigma_{0.2}$ of 158 MPa and ultimate tensile strength (UTS) of 206 MPa, respectively. Compare with extruded Mg-6Li-1.2Zn-1.2Y alloy, the extruded Mg-6Li-0.3Zn-0.6Y alloy have high strength but low elongation. This situation is estimated to be caused by particle-like LPSO phase delivering the interface of α and β phases in Mg-6Li-0.3Zn-0.6Y alloy, as mentioned above. The distribution of LPS structure as well as fine $Mg_3Zn_3Y_2$ phase in matrix increases strength. On the other hand, the secondary phase with LPS structure distributed heterogeneously at the grain boundary decrease the elongation.

Table 3.
The mechanical properties of experimental alloys (tested at room temperature)

Alloys	As-cast state			As-extruded state		
	$\sigma_{0.2}$ （MPa）	UTS (MPa)	Elongation (%)	$\sigma_{0.2}$ （MPa）	UTS (MPa)	Elongation (%)
Mg-6Li-0.3Zn-0.6Y	102	163	10	180	225	18
Mg-6Li-1.2Zn-1.2Y	110	152	13	158	206	28

4. Conclusions

1) As-cast Mg-6Li-0.3Zn-0.6Y alloy is composed of α-Mg+W-$Mg_3Zn_3Y_2$+X-$Mg_{12}ZnY$+β-Li. But there is no X-phase in as-cast Mg-6Li-1.2Zn-1.2Y alloy. Therefore, it indicates that the X-$Mg_{12}ZnY$ exist in Mg-Li-Y-Zn alloys with relative high Y/Zn ratio.

2) The grain size of specimen is greatly refined and the precipitated phases are crushed into block-like and distributes uniformly at the interface of α-Mg/β-Li after the hot extrusion. Based on the results of calculation, the average grain size before and after extrusion is refined from 80 μm to 15 μm. The α-Mg phase is elongated, while β-Li phase exhibits equiaxed morphology with a grain size of smaller than 5 μm through extrusion.

3) The mechanical properties of specimen are both improved after extrusion. The ultimate tensile strengths of extruded Mg-6Li-0.3Zn-0.6Y and Mg-6Li-1.2Zn-1.2Y alloys are improved to 225 MPa and 206 MPa respectively, which are enhanced by 38% and 35% separately compared with those of as-cast specimen. And the corresponding elongations reach to 18% and 28%, respectively.

4) It reveals that LPSO phases which only exist in Mg-Li-Y-Zn alloys with relative high Y/Zn ratio can enhance the strength of the alloy as solid solution strengthening phase. With the increase in both yttrium and zinc contents, the elongation of the alloy increases correspondingly while the UTS shows no obvious drop.

Acknowledgments

References

[1] Cheng, Z.Y. & Li, Z.Q. (2011). Hot deformation behavior of an extruded Mg–Li–Zn–RE alloy. *Materials Science and Engineering A*. 528, 961-966.

[2] Braszczyńska-Malik, K.N. (2014). Some mechanical properties of experimental Mg-Al-Re-Mn magnesium alloys. *Archives of Foundry Engineering*, 14, 13-16.

[3] Gasior, W., Moser, Z. & Zakulski, W. (1996). Thermodynamic studies and the phase diagram of the Li-Mg system. *Metallurgical and Materials Transactions A*. 27(9), 2419.

[4] Mahata, A. & Sikdar, K. (2016). Molecular dynamics simulation of nanometer scale mechanical properties of hexagonal Mg-Li alloy. *Journal of Magnesium and Alloys*. 4, 36-43.

[5] Chang, T.C. & Wang, J.Y. (2009). Mechanical properties and microstructures of various Mg–Li alloys. *Materials Letters*. 60, 3272-3276.

[6] Feng, S. & Liu, W.C. (2017). Effect of extrusion ratio on microstructure and mechanical properties of Mg–8Li–3Al– 2Zn–0.5Y alloy with duplex structure. *Materials Science & Engineering A*. 692, 9-16.

[7] Zhang, J.Y. & Xu, M. (2009). Effect of Gd addition on microstructure and corrosion behaviors of Mg–Zn–Y alloy. *Journal of Magnesium and Alloys*. 4, 319-325.

[8] Dong, H.W. & Wang, L.D. (2011). Preparation and haracterization of Mg-6Li and Mg-6Li-1Y alloys. *Journal of Rare Earths*. 29, 645-649.

[9] Luo, S.Q. & Tang, A.T. (2011). Effect of mole ratio of Y to Zn on phase constituent of Mg-Zn-Zr-Y alloys. *Transactions of Nonferrous Metals Society of China*. 21, 795-800.